Modeling the Delamination Process During Shear Premixing of Nanoclay/Thermoset Polymer Nanocomposites

T.-D. Ngo,[1] P. M. Wood-Adams,[1] S. V. Hoa,[1] M.-T. Ton-That[1,2]

[1]*Department of Mechanical and Industrial Engineering, Concordia University, Montreal, Quebec, Canada H3G 1M8*
[2]*National Research Council Canada, Industrial Materials Institute, Boucherville, Quebec, Canada J4B 6Y4*

Received 21 April 2010; accepted 14 January 2011
DOI 10.1002/app.34180
Published online 27 April 2011 in Wiley Online Library (wileyonlinelibrary.com).

ABSTRACT: As shear premixing is an important process for the dispersion of nanoclays in polymeric resins, this article studies the effect of temperature, duration, speed of premixing, and also the interlamellar spacing of clay platelets on the dispersion of organoclay in epoxy by using a high speed premixing technique which can generate high shear. The quality of dispersion and intercalation/exfoliation of organoclay in epoxy after premixing (before adding hardener) was analyzed by means of X-ray diffraction (XRD) and rheological measurement. The dispersion and intercalation/exfoliation of organoclay in the epoxy nanocomposites (ENCs) after curing were characterized by TEM. The results illustrate that the intercalation/exfoliation of organoclay in epoxy at the premixing step is very much depending on the premixing parameters. This article also presents a model which takes into account the parameters such as the interlamellar spacing of clay platelets, the viscosity of the epoxy-clay mixtures, and the velocity of the mixer to explain their effect on the dispersion of clay in epoxy resin. The study focuses on the flow of epoxy clay in the high shear mixer to describe a model for predicting the processing conditions necessary for achieving delamination of the clay layers. Experimental results on the dispersion of clay are also provided to validate the model. The model provides a guide for the premixing parameters necessary to separate the clay layers. © 2011 Wiley Periodicals, Inc. J Appl Polym Sci 122: 561–572, 2011

Key words: nanoclay; nanocomposites; thermoset; shearing effect; high speed; dispersion; intercalation and exfoliation; model for dispersion

INTRODUCTION

Several studies on the effect of shear force on dispersion and properties of thermoplastic nanocomposites have been reported in the literature based on shearing devices such as extruders, mixers, and ultrasonicators.[1–7] However, the mixing devices used for uncured thermoset systems are different from these devices and the rheological properties of uncured thermoset resins are very different from those of thermoplastic polymers. Therefore, the effect of shear flow on the dispersion of nanoclays in thermoset polymers has not been studied in detail, especially at the premixing stage where the clay and epoxy are combined before curing. The term "dispersion" is used to refer to the complete process of incorporating the powder into a liquid medium such that the final product consists of fine particles distributed throughout the medium. The dispersion of fine particles is normally termed colloidal if at least one dimension of the particles lies between 1 nm and 1 μm. Solid particles dispersed in a liquid form a suspension. In many practical uses of powders the primary particle size is sufficiently small such that further subdivision is unnecessary. However in the dry state, the powder usually contains aggregates of primary particles which are attached to other aggregates and/or primary particles forming agglomerates. Aggregates may require considerable energy to break down to the point when the surface of each primary particle is available to the wetting liquid. There are at least three major types of interaction involved in colloidal particles, namely the London-Van der Waals forces of attraction, the Coulombic force (repulsive or attractive) associated with charged particles, and the repulsive force arising from solvation, or adsorbed layers. Nano-layered silicates, which are lamellar nano-particles, are among the most interesting for the production of polymer nanocomposites. The commonly used layered silicates belong to the same general family of 2 : 1

**Present address:* National Research Council Canada, Industrial Materials Institute.
Correspondence to: T.-D. Ngo (tridung.ngo@cnrc-nrc.gc.ca).
Contract grant sponsors: Vietnamese Government, Natural Sciences and Engineering Research Council of Canada.

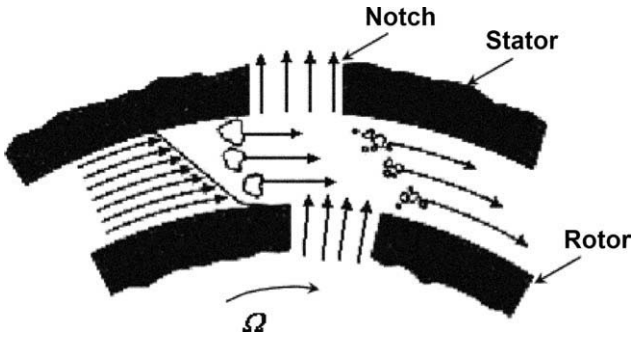

Figure 1 The mixer flow geometry.

layered- or phyllosilicates.[1,5,8–13] Their crystal structure consists of layers made up of two tetrahedrally coordinated silicon atoms fused to an edge-shared octahedral sheet of either aluminum or magnesium hydroxide. The layer thickness is around 1 nm, and the lateral dimensions of these layers may vary from 30 nm to several microns or larger, depending on the particular layered silicate. Stacking of the layers leads to a regular Van der Waals gap between the layers called the interlayer or gallery. Therefore, the Van der Waals interaction represents to the energy barrier to clay exfoliation[8–13] and is the most important force to be considered here.

In the preparation of epoxy nanocomposites, two steps are involved: premixing and mixing. Premixing is the mixing of nanoclay in the liquid epoxy without the presence of the curing agent, and mixing means the incorporation of the curing agent into the mixture of clay and epoxy. As shear flow is a very important process for the forming of thermosetting nanocomposites, this article studied the effect of different parameters on the dispersion of the epoxy/clay nanocomposite materials made by this high speed premixing technique, a systematic study of the effect of premixing parameters (temperature, speed, duration of premixing, and level of clay intercalant) was undertaken. This article also develops and validates a model that allows the determination of the critical process conditions for achieving delamination of the clay layers.

EXPERIMENTS

The resin selected for this study was EPON™ 828, from Resolution Performance Products LLC (Houston, TX). This was cured with the polyoxypropylene diamine hardener Jeffamine® D-230 from Huntsman LLC (The Woodlands, TX) at a level of 32 phr. Organoclays recommended for use with amine-cured epoxy systems was used, namely Cloisite® 30B (montmorillonite treated with methyl tallow bis(2-hydroxyethyl) quaternary ammonium) from Southern Clay Products (Gonzales, TX), Nanomer® I.30E (montmorillonite treated with octadecyl amine, a primary amine base) from Nanocor (Arlington Heights, IL). Henceforth the hardener and clays are designated in shortened form as D230, C30B, and I30E, respectively. Also a new organoclay was used where the clay was intercalated with a long chain amine intercalant (polyoxypropylenetriamine, M_w of 2000). The organoclays and epoxy were premixed at different conditions such as temperature, speed, and time. For this study a high speed mixer has been used with flow geometry as shown in Figure 1. These organoclays were dispersed in the epoxy resin at a level of 2.69% by weight, which leads to a loading of 2% by weight after addition of hardener and curing. Rheological measurement at room temperature for epoxy-clay suspensions after premixing was performed on a Brookfield CAP2000+ viscometer for the epoxy and the epoxy-organoclay suspensions using cone and plate geometry at room temperature. To evaluate the intercalation/exfoliation of the nanoclay in the polymer matrix, X-ray diffraction (XRD) patterns were obtained on the samples with a Bruker Discover 8 powder X-ray diffractometer with Cu Kα radiation. For clay dispersion at the nano-level, ultra-thin (50–80 nm) sections of nanocomposite samples were prepared with a cryo-ultramicrotome and supported on a copper 200 mesh grid for observation with a Hitachi H9000 transmission electron microscope (TEM). Samples were cured at 120°C for 2 h, with subsequent post cure at 140°C for 2 h.

RESULTS

Figure 2 shows the relevant experimental results for the X-ray diffraction curves on the organoclay and mixture of epoxy-organoclay samples after being premixed at different speeds and temperatures. The *d*-spacing of organoclay in epoxy-organoclay mixture is shown in Figure 3. One can see the C30B has the original *d*-spacing of 1.85 nm. The results show roughly the same distance between the clay sheets for the mixtures of epoxy-organoclay, even though there is significant increase in *d*-spacing of the clay from 1.85 nm (for C30B) to 3.80 nm (mixtures). The same distance between the clay sheets (*d*-spacing) for epoxy-organoclay mixture which was prepared at room temperature and 120°C can also be seen. It seems that the diffusion of epoxy molecules into clay galleries almost reached equilibrium and the premixing is not further separate the clay sheets.

The effects of premixing duration together with temperature and speed on the intercalation/exfoliation of clay in epoxy were also investigated. X-ray diffraction results on the *d*-spacing of the epoxy and C30B prepared by high speed of premixing at different temperatures of room temperature, 120°C, 180°C

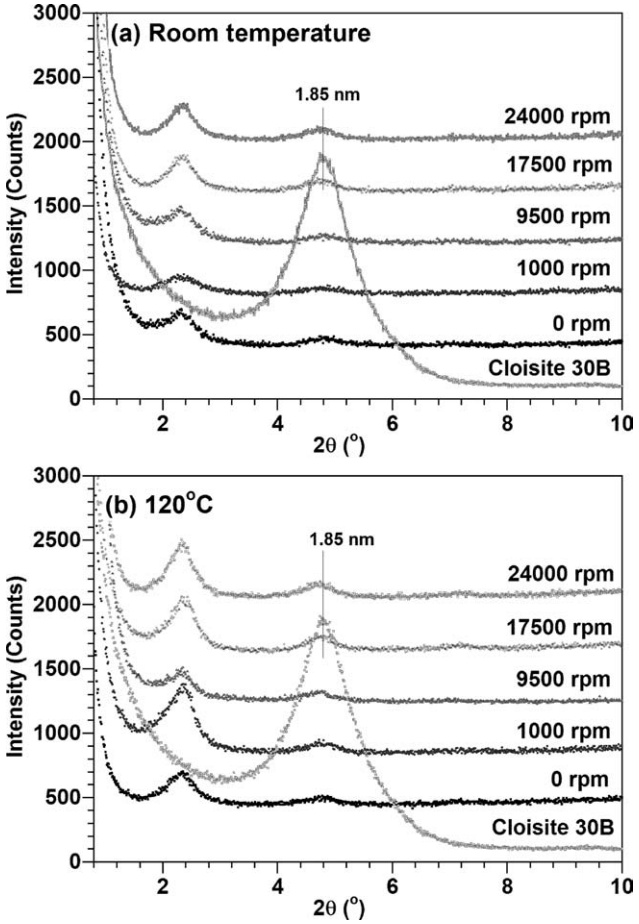

Figure 2 X-ray diffraction curves of C30B and its EPON828-C30B mixtures after being pre-mixed at different speeds: (a) room temperature and (b) 120°C.

and different speeds of 9500, 17,500, and 24,000 rpm at 2, 4, 10, 20, 30, 45, and 60 min are illustrated in Figure 4. Again, it can be seen that the clays have been well intercalated by the epoxy resin. As a consequence, there is roughly the same distance between the clay sheets or just a very slight increase in the *d*-spacing with increasing duration of premixing. The *d*-spacing also does not significantly change even when the mixture was premixed up to 24 h. It can be concluded then that the mixing duration does not significantly affect the exfoliation of clay in epoxy resin at premixing step. For more information on the dispersion of clay and the effect of premixing parameters, refer to Refs. 6 and 7.

The viscosity of the epoxy EPON828 and its mixtures with C30 at different temperatures was examined with a Brookfield Digital Viscometer Model DV-II+. The results are shown in Figure 5. As expected, at the same temperature the EPON828 has the lowest viscosity compared to its mixtures with C30B. The results also show that the viscosity of EPON828-C30B mixtures after premixing at high temperature of 120°C for 60 min is slightly higher than EPON828-C30B mixtures after premixing at room temperature for 60 min.

The *d*-spacing of C30B and I30E in liquid epoxy resin after being premixed were examined by X-ray diffraction and the results are shown in Figure 6(a,b). C30B has the original *d*-spacing of 1.85 nm, whereas I30E has the original *d*-spacing of 2.38 nm. It appears that in the epoxy-clay mixtures, the *d*-spacing is around 3.72–3.81 nm for both types of clay. The results indicate that the intercalation is very similar for C30B and I30E after they have been added to epoxy resin. It seems that with *d*-spacing of clay of up to 2.38 nm, the exfoliation is not achievable in this mixer. To further investigate the effect of initial *d*-spacing on the exfoliation of clay into epoxy, we have incorporated a clay that was intercalated with a long chain amine intercalant (polyoxypropylenetriamine, M_w of 2000) prior to premixing with the epoxy. This intercalant provided an initial *d*-spacing of around 6.0 nm [Fig. 6(c)], and an exfoliated clay-epoxy system was obtained after premixing at 24,000 rpm for 15 min in the high shear mixing device. The results show that there is no

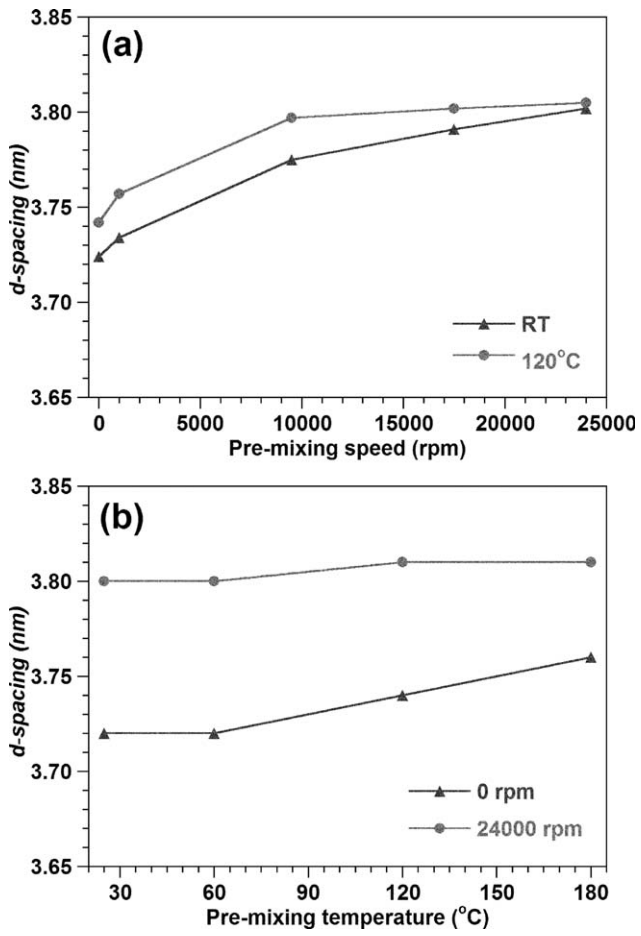

Figure 3 *d*-spacing of EPON828-C30B mixtures after premixing at different speeds and temperatures.

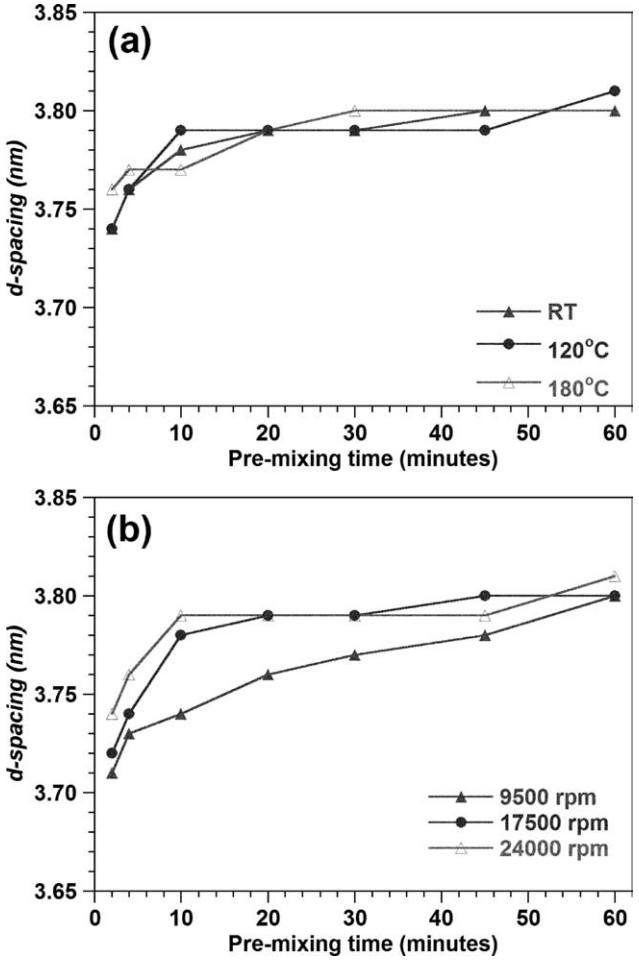

Figure 4 *d*-spacing of EPON828-C30B mixtures after premixing at different times, temperatures and speeds.

peak on the XRD curve for this clay [Fig. 6(c)] after premixing.

The TEM images of the epoxy nanocomposites for different clays are shown in Figure 7. Again, they confirm that exfoliation was not achieved for clay C30B and I30E, where the *d*-spacing of clay observed by TEM is about 4 nm or less, and the layers are still in stacks [Fig. 7(a,b)]. On the other hand, the *d*-spacing of the polyoxypropylenetriamine intercalated clay observed by TEM is 10 nm or more, and also the layers are no longer arranged in stacks [Fig. 7(c)].

MODELING THE DELAMINATION PROCESS

From the experimental results, we find that the layer separation for the commercial clays after the premixing step is around 3.8 nm regardless of the mixing conditions and exfoliation is not achieved until after curing. Exfoliation was achieved after the premixing step in the case of the in-house prepared clay with the long chain amine intercalant where the original *d*-spacing of 6.0 nm. The question to be answered here is why one is not able to achieve the exfoliation of clay at the premixing step for C30B and I30E using the existing equipment? We note that result is not unique to our system and other similar systems have been reported in the literature showing that the clay layer separation is always around 3.5–3.9 nm or even smaller.[1–5] Also we are interested to determine mixing conditions that would be required to obtain exfoliation of clay. To answer these questions, the flow of the epoxy and clay mixture under high speed premixing was examined from a theoretical point of view.

VAN DER WAALS FORCES BETWEEN TWO PARTICLES OR MACROSCOPIC BODIES

The London Van der Waals attractive forces are based on electronic interactions; due to the interaction of dipoles within the particles. These may be permanent dipoles of polar particles or dipoles that may be induced in polarizable nonpolar particles.[14–16]

The origin of dispersion interactions can be explained from the following argument. For nonpolar atoms, such as rare gases, the time-average dipole moment is zero. However, at any instant there exists an instantaneous dipole moment determined by the location of the electrons around the nucleus. This dipole generates an electric field, which in turn induces a dipole in nearby neutral atoms. The resulting interaction gives rise to an attraction force between the two atoms whose time average is finite. The same argument applies for the attraction of two nonpolar molecules. In 1933 London derived an expression for the attraction between a pair of atoms by solving the Schrödinger equation. He modeled each of the atoms as a charged harmonic oscillator with a characteristic frequency ν

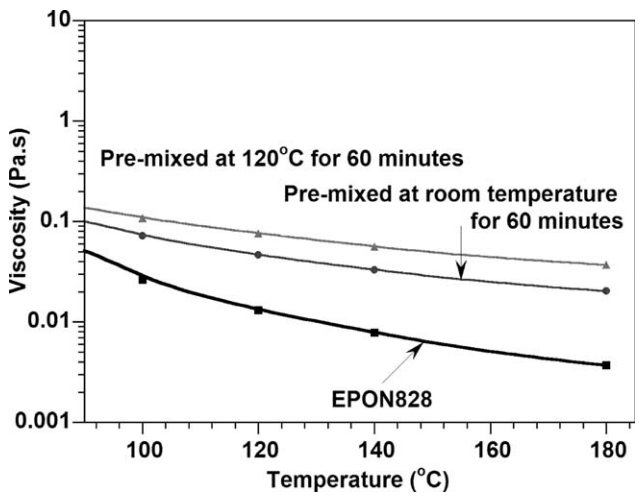

Figure 5 The relation between temperature and viscosity of epoxy and its mixtures with C30B after being pre-mixed at room temperature (RT) and 120°C at 60 min.

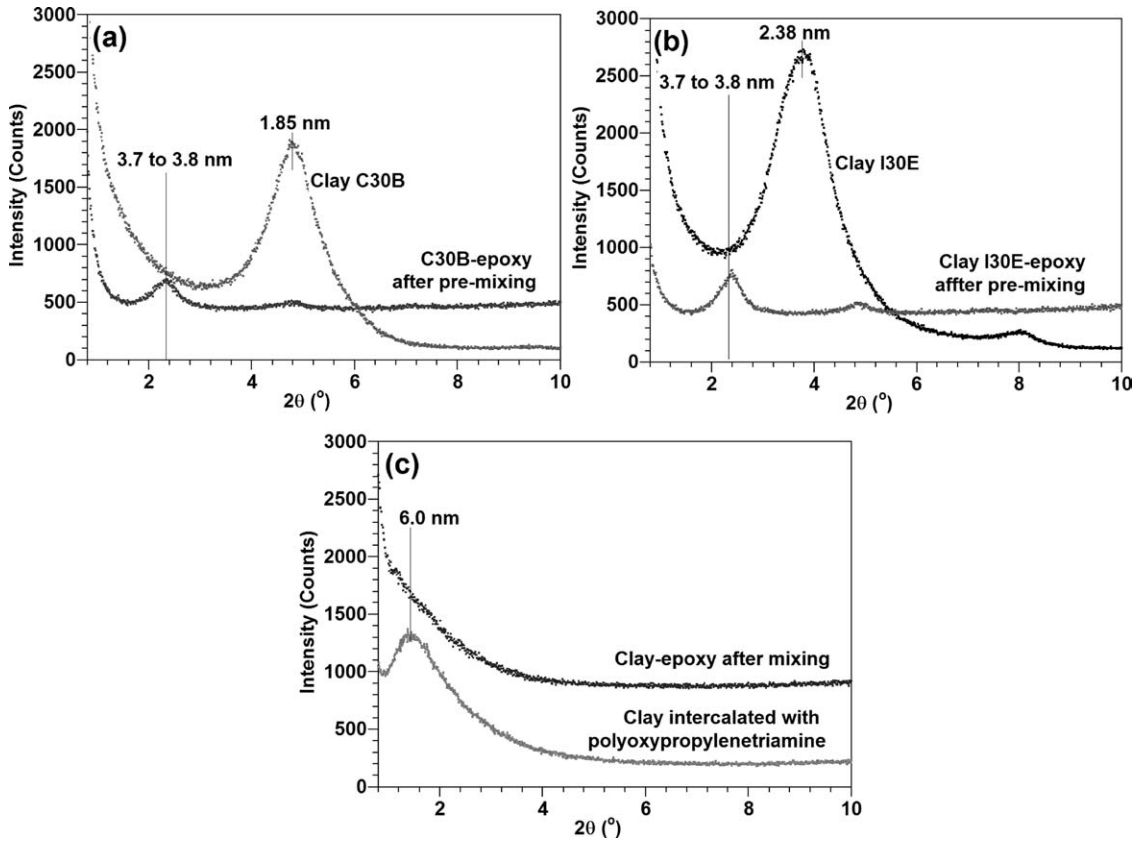

Figure 6 X-ray diffraction curves of EPON828-clay mixtures with different clays which has different original *d*-spacing of (a) 1.85, (b) 2.38, and (c) 6.0 nm.

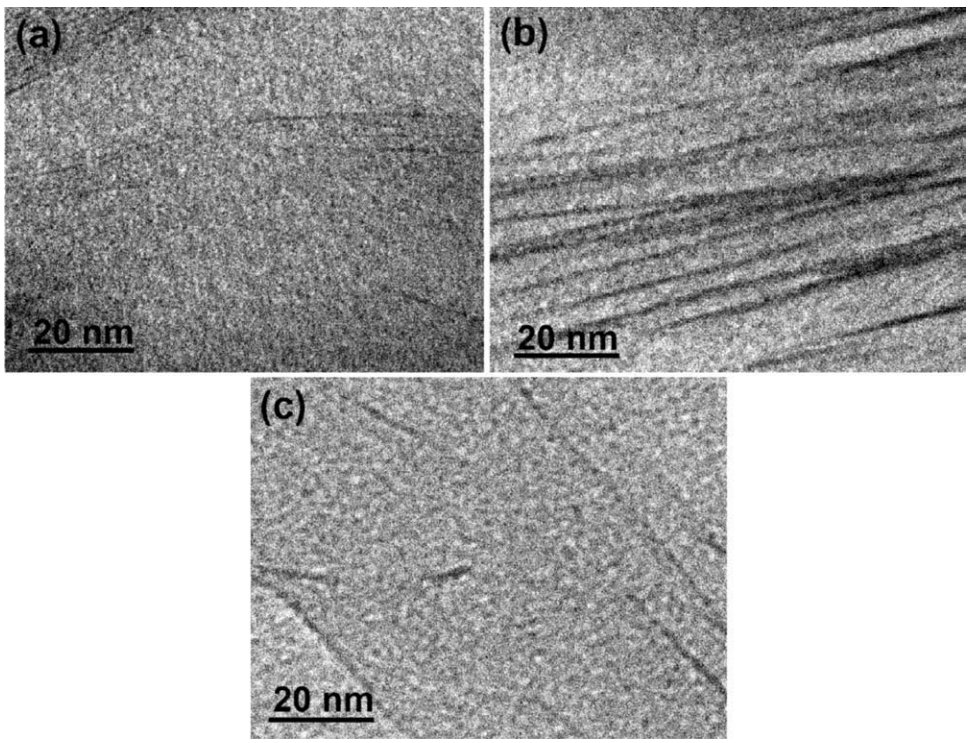

Figure 7 TEM photo of nanocomposites with different clays which has different original *d*-spacing of (a) 1.85, (b) 2.38, and (c) 6.0 nm.

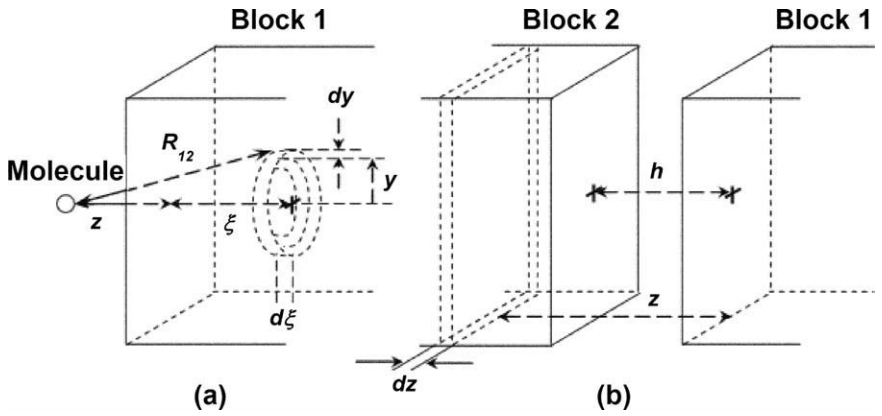

Figure 8 Schematic for coordinates (a) between a molecule and a block, (b) two blocks.

and obtained attractive interaction energies between two similar atoms.[14]

$$E(R_{12}) = -\frac{3}{4}\frac{a^2 h_p \nu}{(4\pi\varepsilon_0\varepsilon_r)^2 R_{12}^6} \tag{1}$$

and for two dissimilar atoms:

$$E(R_{12}) = -\frac{3}{2}\frac{a_1 a_2}{(4\pi\varepsilon_0\varepsilon_r)^2 R_{12}^6}\left(\frac{h_p \nu_1 \nu_2}{\nu_1 + \nu_2}\right) \tag{2}$$

In these equations h_p is Planck's constant and $h_p\nu$ generally equals the ionization energy of the atoms, a is the polarizability, R_{12} is the intermolecular distance, ε is relative dielectric permittivity, or the dielectric constant, ε_0 is the electric permittivity of vacuum ($\varepsilon_0 = 8.854 \times 10^{-12}$ C^2 J^{-1} m^{-1}, coulombs^2 per joule per meter). Dispersion forces, like gravitational forces, operate between all atoms or molecules.

Next we consider interaction potentials and forces between two particles that contain many atoms. If we assume pairwise additivity between molecules, we can sum over all possible pairs, one molecule in each body, to obtain the dispersion force between two macroscopic bodies or particles. The discussion that follows represents the two particles as two blocks with planar surfaces of infinite lateral dimensions separated by a distance h in vacuum ($\varepsilon_r = 1$). In calculating the attractive interaction between pairs of molecules, Eq. (1) is used. Consider first the interaction between a single molecule (or atom) and a block (Block 1) where the normal distance from the molecule to the surface of the block is z, as shown in Figure 8.

In a slice d_z we will have $(\rho N_{AV}/M)d_z$ molecules per unit area, and the interaction potential due to that element per unit area will be

$$dE(z) = -\left(\frac{\rho N_{AV}}{M}\right)^2 \frac{C_{disp}\pi}{6}\frac{dz}{z^3} \tag{3}$$

where $C_{disp} = (3/4)a^2 h_p \nu/(4\pi\varepsilon_0)^2$, $\rho N_{AV}/M$ (ρ is density; M is molecular weight) is the number of molecules per unit volume in the block, N_{AV} is Avogadro's number

With z from h to ∞, the attraction interaction energy per unit surface area of particles $E_{att,p}(h)$ is:

$$E_{att,p}(h) = -\left(\frac{\rho N_{AV}}{M}\right)^2 \frac{C_{disp}\pi}{12}\frac{1}{h^2} = -\frac{H_{11}}{12\pi}\frac{1}{h^2} \tag{4}$$

$$H_{11} = \left(\frac{\rho N_{AV}}{M}\right)^2 C_{disp}\pi^2$$

In this equation, H_{11} is called the Hamaker constant, a material constant that measures the attraction between two particles of material in vacuum.

Using the same approach, the attraction energy holding two thin plates together is given by[14,15]:

$$E_A|_h = -\frac{H_{11}}{12\pi}\left[\frac{1}{h^2} + \frac{1}{(h+2\delta)^2} - \frac{2}{(h+\delta)^2}\right] \tag{5}$$

where h is the distance between the surfaces of the plates, δ is the thickness of the plate (assuming that both plates are of the same thickness).

THEORETICAL MODEL OF FLOW OF EPOXY/CLAY MIXTURE IN HIGH SPEED MIXING

The ultimate goal is to determine if it is theoretically possible to separate two layers of clay under specific mixing conditions. The mixer flow geometry (cross section) was shown in Figure 1. In this schematic, the dots represent the particles in the fluid. The mixer consists of two concentric cylinders, each containing several small notches as shown. The inner cylinder (radius R_i) spins at a constant angular velocity, Ω. The centrifugal force moves the liquid from the middle of the inner cylinder to the gap between the two cylinders where it is sheared before

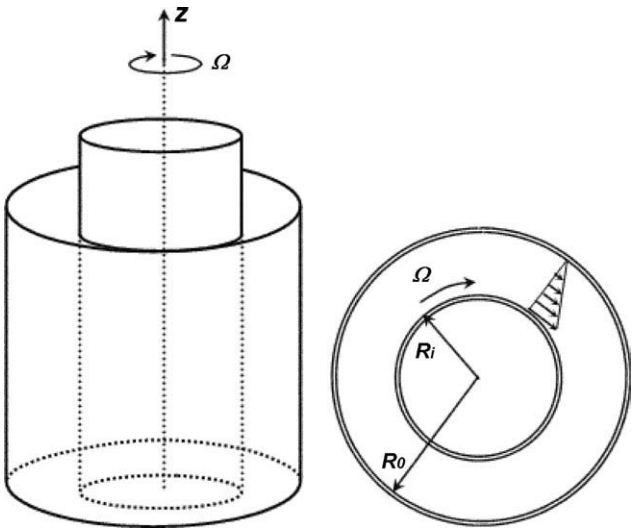

Figure 9 Flow between rotating cylinders.

exiting through the notches in the outer cylinder (radius R_o).

To simplify the flow of the epoxy and clay mixture in this mixer, the mixer geometry can be considered as in Figure 9. That is, a tangential annular flow of a fluid between two concentric cylinders when the inner cylinder is turning. The inner cylinder spins at a constant angular velocity, Ω.

We consider an incompressible, isothermal, Newtonian fluid in steady, laminar flow between the two coaxial cylinders, whose inner and outer wetted surfaces have radii of R_i and R_o, respectively. We assume additionally that the effects of the clay particles on the flow are negligible (the clay loading in this study is 2% weight). In steady laminar flow, and neglecting the effect of gravity, the fluid is expected to travel in a circular motion; only the tangential component of velocity exists. The radial and axial components of velocity are assumed to be zero; so $\upsilon_r = 0$ and $\upsilon_z = 0$. We note that this is strictly correct for Reynolds number, $Re = \Omega\rho R_i\,(R_o - R_i)/\mu$, below a critical value which for our gap $(R_o - R_i)$ is ~ 200.[17] We will address this issue further when we apply the model. Additionally, by neglecting end effects we find that the flow variables do not vary in the z direction. By applying the continuity equation and the equation of motions for an incompressible, Newtonian fluid and incorporating the previous assumptions one can derive the velocity profile[18,19]:

$$\upsilon_\theta = \frac{R_i^2 R_o^2 \Omega}{R_o^2 - R_i^2}\left(\frac{1}{r} - \frac{r}{R_o^2}\right) \tag{6}$$

where r *is* the radial component in cylindrical coordinates.

In the above form, the term on the right-hand-side of the equation corresponds to the velocity profile when the outer cylinder is stationary and the inner cyslinder is rotating with an angular velocity, Ω.

DETERMINATION OF VELOCITY NEEDED TO DISPERSE THE CLAY SHEETS

The force on a surface with unit normal $\hat{n}$ is given by

$$\underline{F} = A\hat{n} \cdot \underline{\underline{\Pi}} \tag{7}$$

where A is the surface area of clay, $\underline{\underline{\Pi}}$ is the total stress tensor, and $\hat{n} \cdot \underline{\underline{\Pi}}$ is the stress vector acting on an area A with normal $\hat{n}$. Considering the geometry in Figure 10 we develop the following relation for the surface normal unit vector:

$$\hat{n} = \begin{pmatrix} \sin\alpha \\ \cos\alpha \\ 0 \end{pmatrix} \tag{8}$$

The force vector acting on the surface of the clay particle due to the extra stress is:

$$\underline{F} = A\hat{n} \cdot \underline{\tau} \tag{9}$$

When combined with the velocity profile and the Newtonian constitutive equation the above equation gives:

$$\underline{F} = A\left(2\mu\frac{R_i^2 R_o^2}{R_o^2 - R_i^2}\Omega\frac{1}{r^2}\right)[\cos\alpha \quad \sin\alpha \quad 0] \tag{10}$$

We are interested in the force tending to separate the two layers in shear shown in Figure 11 which is:

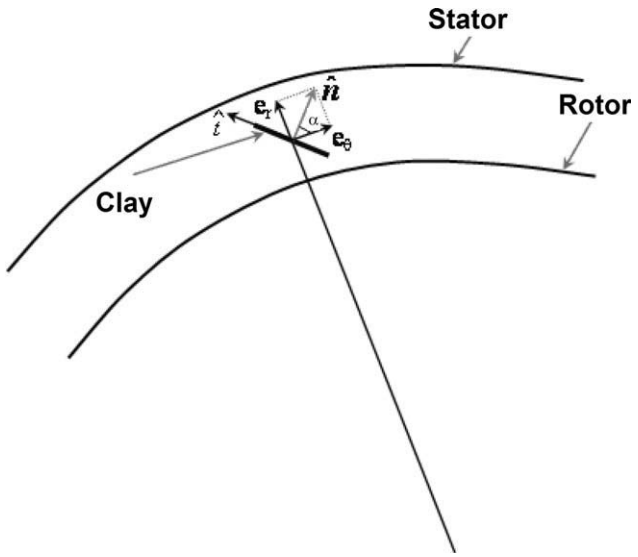

Figure 10 Flow of epoxy-clay mixture between rotating cylinders.

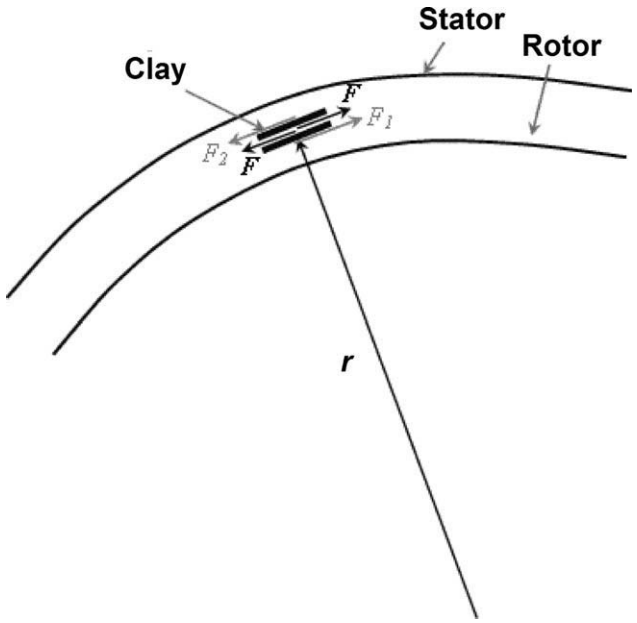

Figure 11 Flow of epoxy-clay mixture between rotating cylinders. F1 and F2 are the forces applied on the surfaces of a particle consisting of two layers due to the shear flow. They are not exactly equal because of the thickness of the particle. In this analysis we neglect the small difference between $F1$ and $F2$, assuming $F = F1 = F2$.

$$F = \underline{F} \cdot \hat{t} = A\left(2\mu \frac{R_i^2 R_o^2}{R_o^2 - R_i^2}\Omega \frac{1}{r^2}\right)\left(\cos^2\alpha - \sin^2\alpha\right) \quad (11)$$

and the force tending to separate the two layers in the surface normal direction is:

$$F = \underline{F} \cdot \hat{n} = A\left(4\mu \frac{R_i^2 R_o^2}{R_o^2 - R_i^2}\Omega \frac{1}{r^2}\right)(\sin\alpha\cos\alpha) \quad (12)$$

From Figure 11 it is clear that the particles will be rotating around their center lines because of the unbalanced moment couple due to $\underline{F}_1 = -\underline{F}_2$. This is a well known behavior exhibited by particles in dilute suspensions. The rotation of particles in dilute non-Brownian suspensions continues indefinitely under shear flow. It is only under either (1) the conditions of significant particle-particle interactions (i.e., jamming) or (2) conditions of significant Brownian behavior that this rotation stops (or slows). We recall that our model is built under the assumption that the particles have a negligible effect on the flow of the liquid phase. Clearly this assumption is invalid in the case of significant particle-particle interactions. Therefore, our model is only strictly valid when the particles are not jamming and α in the above equation is a function of time. In the case of significant Brownian motion, α will vary randomly with time independent of the shear rate. We consider a suspension to be Brownian if the rate at which the particle moves due to Brownian motion is similar to the rate at which it moves due to the flow. We can evaluate this exactly using the rotational Peclet number[20]:

$$Pe = \frac{R_i\Omega}{R_0 - R_i}\left(\frac{1}{D_r}\right) \quad (13)$$

In the above equation D_r, the rotary diffusivity, is given by the following equation for a circular disk-like particle of diameter d[20]:

$$D_r = \frac{3k_B T}{4\mu_S d^3} \quad (14)$$

where k_B is Boltzmann's constant, T is the absolute temperature, and μ_S is the viscosity of the suspending fluid. For our case, at room temperature $D_r \cong 30$ 1/s and the Peclet number is $\sim$ 14,000. Since $Pe \gg 1$ we can consider our particles to be non-Brownian. This means that we expect the angle α to be the following specific function of time[19]:

$$\tan(\alpha - 90) = p\tan\left[\left(\frac{R_i\Omega}{R_0 - R_i}\right)\left(\frac{t}{p + 1/p}\right)\right] + \tan(\alpha_0 - 90) \quad (15)$$

where t is time, α_0 is the angle at time $t = 0$, and the aspect ratio, p, is:

$$p = \frac{2\delta + h}{L} \quad (16)$$

Equation 15 results from the integration of the equation of motion for a non-Brownian particle in a shear flow field.[21] For our particle consisting of two layers, the geometrical parameters for the clay layers are defined in Figure 12. In the following analysis we are going to consider the maximum force F which occurs at $\alpha = 0^\circ$ for shear direction and $\alpha = 45^\circ$ for the surface normal direction, while remembering that each particle will only experience this force during part of its rotation period, P, which is given by the equation below.[22]

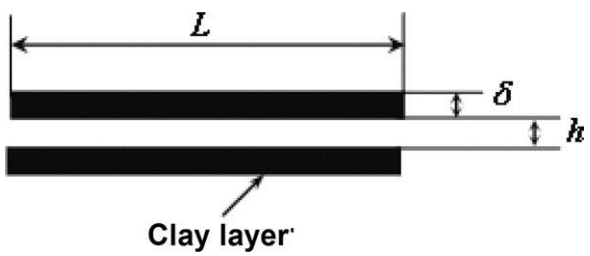

Figure 12 Dimensions of clay particles.

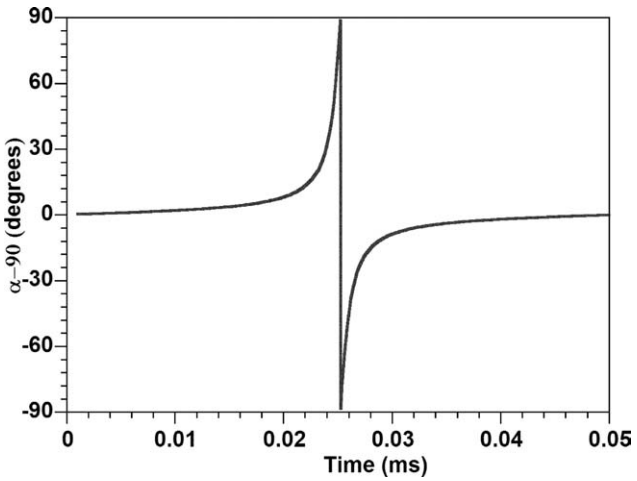

Figure 13 Relationship between α and time.

$$P = \frac{\pi(R_0 - R_i)}{R_i\Omega}(p + 1/p) \tag{17}$$

We now move on to consider the requirements for delamination. To be able to delaminate the clay we need to have $F - F_c \geq 0$ or $F \geq F_c$, where F is the force imposed on clay by shearing (see Fig. 4) and F_c is the force holding the clay together. The limiting case of $F = F_c$ is:

$$A\left(2\mu\frac{R_i^2R_o^2}{R_o^2 - R_i^2}\Omega\frac{1}{r^2}\right)(\cos^2\alpha - \sin^2\alpha) = F_c \tag{18}$$

for the shear direction or

$$A\left(4\mu\frac{R_i^2R_o^2}{R_o^2 - R_i^2}\Omega\frac{1}{r^2}\right)(\sin\alpha\cos\alpha) = F_c \tag{19}$$

for the surface normal direction.

The maximum shearing force experienced by a clay particle will occur at $r = R_i$ and $\alpha = 0°$ and the maximum stretching force will occur at $r = R_i$ and $\alpha = 45°$. The magnitudes of these maximum forces are identical. The relationship between α and time is shown in Figure 13 [from Eq. (15)]. This analysis indicates that most of time the clay particles are experiencing stretching forces rather than shearing forces.

Therefore by substituting the geometrical conditions for maximum force specified above we find the minimum rotational speed that will allow clay layers to be separated:

$$\Omega_{\min} = \frac{F_c}{A\left(2\mu\frac{R_o^2}{R_o^2 - R_i^2}\right)} \tag{20}$$

The attraction energy holding two clay sheets together from Eq. (5) is:

$$E_A|_h = -\frac{H_{11}}{12\pi}\left[\frac{1}{h^2} + \frac{1}{(h+2\delta)^2} - \frac{2}{(h+\delta)^2}\right] \tag{21}$$

where the Hamakar constant H_{11} is 7.8×10^{-20} J,[23–25] h is the distance between the surfaces of the sheets, δ is the thickness of the clay sheets as shown in Figure 12.

We now assume that the Van der Waals forces holding the two platelets together are not directional, giving the following equation for the total attractive force:

$$F_c|_h = \frac{dE_A}{dh}(Af) = -\frac{H_{11}}{12\pi}\left[\left(\frac{4}{(h+\delta)^3}\right) - \left(\frac{2}{h^3}\right) - \left(\frac{2}{(h+2\delta)^3}\right)\right](Af) \tag{22}$$

where f is the ratio between the attractive area (area where the clay sheets interact) and total area (total surface area of clay sheet). Practically speaking this means that we assume that the force to separate the two plates in shear is the same as the force required to separate the plates in the surface normal direction. This assumption is not strictly correct because it applies only for particles having spherical symmetry which our plates clearly do not have. To justify this approximation, we recall that the magnitude of the maximum shear force (occurring at $\alpha = 0°$) is equal to the magnitude of the maximum normal force (occurring at $\alpha = 45°$). Therefore whether we are considering that the delamination occurs in tension or in shear our analysis gives the same results. Finally we present F_c and E_A in terms of the parameters listed above:

$$F_c|_h = \frac{dE_A}{dh}(A) = -\frac{H_{11}}{12\pi}\left[\left(\frac{4}{(h+\delta)^3}\right) - \left(\frac{2}{h^3}\right) - \left(\frac{2}{(h+2\delta)^3}\right)\right](A) \tag{23}$$

Now we combine this with Eq. (20) under the conditions for maximum force to find:

$$\Omega_{\min} = \frac{-\frac{H_{11}}{12\pi}\left[\left(\frac{4}{(h+\delta)^3}\right) - \left(\frac{2}{h^3}\right) - \left(\frac{2}{(h+2\delta)^3}\right)\right]}{\left(2\mu\frac{R_o^2}{R_o^2 - R_i^2}\right)} \tag{24}$$

Equation 24 shows relationship in between minimum rotational speed and viscosity, interlamellar

spacing h, thickness δ of clay sheets, radii of inner R_i and outer R_o wetted surfaces between the two coaxial cylinders. The relationship between those parameters can be used for prediction of their conditions necessary for achieving delamination of the clay layers.

APPLICATION OF THE ABOVE SOLUTION TO THE EXPERIMENTAL SYSTEM

The question is why one is not able to achieve the exfoliation of clay at the premixing step and thus also in the nanocomposite. Consider a high speed mixer (as shown in Fig. 1) with the following dimensions: $R_i = 9$ mm, $R_o = 9.5$ mm, and Ω ranges from 6500 to 24,000 rpm. Consider also that the clay sheets are plates with a side length of $L = 100$ nm and thickness δ of 0.96 nm. We recall that in order for the flow model to be exactly correct then the Reynolds number should be less than 200. For our system this corresponds to $\Omega/\mu < 49500\ P\alpha^{-1}s^{-2}$ where Ω is in units of radians s^{-1} and μ is in Pa s^{-1} and for the maximum speed of 24,000 rpm the minimum viscosity for which the flow model is exact is 0.05 Pa s^{-1} For lower viscosities we expect the formation of toroidal vortices and nonzero radial and axial velocities. The radial and axial velocities will however be small fractions of the surface velocity of the rotating cylinder. Therefore even in this case, our estimation of the shear force assuming flow only in the circumferential direction will still be rather close to reality.

The relationship in Eq. (24) between minimum rotational speed and viscosity and interlamellar spacing h is presented in Figure 14. It is clear from this figure that, the larger is the interlamellar spacing of clay before premixing; the lower is the speed of premixing necessary to disperse the clay. For example, with the viscosity of the epoxy-clay suspension at 0.1 Pa s^{-1} (the third curve from the top), if the interlamellar spacing h is 4.0 nm, the minimum velocity that will be needed to separate the clay platelets is at least 82,000 rpm. However if h is 6.0 nm, the minimum velocity will reduce to 14,500 rpm. Also we can observe that the minimum required rotational speed decreases as viscosity increases. With the interlamellar spacing h of 4.0 nm, if the viscosity is 0.01 Pa s^{-1}, the minimum required rotational speed will be 821,000 rpm. However if the viscosity increases to 1.0 Pa s^{-1}, the minimum required rotational speed will reduce to 8210 rpm. Therefore this model can be used as a guide for the parameters including viscosity; rotational velocity and the interlamellar spacing that are needed to separate the clay layers.

Taking into account that the d-spacing of the clay after swelling in epoxy resin is around 3.81 nm

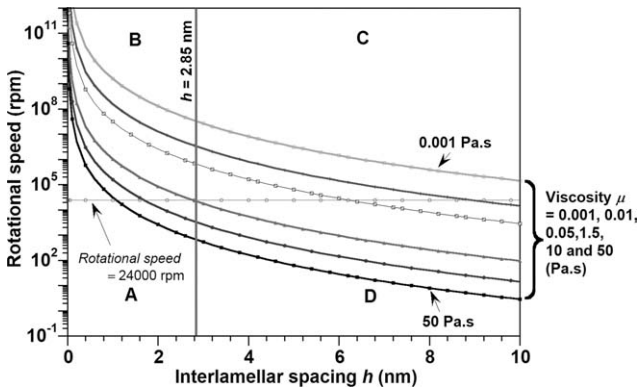

Figure 14 Rotational speed versus interlamellar spacing h.

(XRD of the mixture of Shell EPON828 epoxy resin and organoclay C30B, I30E, and their nanocomposites after curing and the maximum velocity of the homogenizer of 24,000 rpm, the processing space in Figure 14 can be divided into four areas. The horizontal line in this figure represents the velocity of 24,000 rpm (maximum for our mixer) and the vertical line represents the interlamellar spacing h of 2.85 nm (h = d-spacing—δ = 3.81–0.96 = 2.85 nm). These two lines divide the figure into four areas (A, B, C, and D). Because of the limitation in speed (24,000 rpm) and the interlamellar spacing h (2.85 nm) of the clay layers after swelling in epoxy, only area A represents processing conditions sufficient to obtain the exfoliated structure of C30B in the EPON828-C30B system at the premixing step with this homogenizer device. Therefore, with the d-spacing as C30B (1.85 nm) even at the limitation speed of the homogenizer of 24,000 rpm, what ever premixing time, speed, temperature, it seems not possible to obtain an exfoliated epoxy-organoclay mixture as can be seen in Figures 2–4,6(a) and 7(a). This happens also for the case of I30E with the original d-spacing of 2.38 nm as can be seen in Figures 6(b) and 7(b). Practically speaking, it means the viscosity of the EPON828-organoclay system has to be at least 1.5 Pa s^{-1} or the intergallery spacing must be higher than 6.0 nm in order for delamination to occur in the present mixer.

While dispersing the clay with a high speed mixer, we should consider two aspects, first the big clay aggregates are broken down to the smaller aggregates, and then the smaller aggregates are delaminated. Some delamination can also happen during the breaking down of big aggregates. We found that breaking down the big aggregates is easier to achieve than the delamination of clay platelets. There is still work to be done to develop nanocomposites with fine dispersions and exfoliated morphologies. Achieving such morphologies with epoxy-based nanocomposites is a challenge. The

model here deals only with the second aspect. It should be noted here that the viscosity of the epoxy-clay mixtures may increase during the mixing due to the dispersion of clay in epoxy since the spherical clay particle agglomerates are broken down into smaller, higher aspect ratio particles.[6] It may have a certain effect on the delamination of clay platelets as described in Figure 14. By increasing the viscosity of the epoxy-clay suspension, the speed required for delamination of clay can reduce. In addition, premixing temperature and time also need to be considered, since they has a slightly influence on the *d*-spacing,[6,7] and hence on the interlamellar spacing h. This also may help to reduce the velocity needed to separate the clay platelets.

From Figure 5, at temperatures above room temperature, the viscosity of all EPON828-C30B mixtures and pure EPON828 is lower than 0.1 Pa s^{-1}. This value of viscosity is much smaller than 1.5 Pa s^{-1}, therefore according to our model we do not expect to be able to achieve the desired exfoliation of clay at the premixing step. Clearly, if we want to separate the clay by using this equipment for a suspension viscosity around 0.05 Pa s^{-1}, we need to have an initial *d*-spacing of 6.0 nm or more. This can be seen for the case of organoclay was intercalated with a long chain amine intercalant [Figs. 6(c) and 7(c)]. We note the absence of a peak on the XRD curve after premixing, the *d*-spacing of clay observed by TEM is 10 nm or more, and also the clay layers are no longer arranged in stacks; all of which validate our model. In other words, to achieve the delamination of clay with this mixer, we need to increase the clay layer separation by another process prior to premixing.

Finally, the present model can also be used to design a new mixer to give the desired shearing force. For example, if we examine Eq. (24) it is clear that by decreasing the gap between the concentric cylinders in the mixer we can decrease the minimum required rotational speed. If we assume a viscosity of 0.05 Pa s^{-1} and an R_o of 9.5 mm we find that $R_i =$ 9.33 mm (instead of 9.0 mm) is sufficient to reduce the minimum speed for delamination [Eq. (24)] to 24,000 rpm.

CONCLUSIONS

The dispersion and intercalation/exfoliation of organoclay in epoxy by using a high speed premixing technique have been studied. To obtain a well dispersion, intercalation/exfoliation of clay in epoxy, the temperature, duration, speed of premixing and also the interlamellar spacing of clay platelets need to be taken into account. A model of flow in a concentric cylinder high shear mixer was developed and applied to predict the processing conditions necessary for achieving delamination of the clay layers. The model provides a useful tool for determining the required processing parameters to separate the clay layers in thermosetting polymers. To separate the clay by using the mechanical mixer, in general or high shear mixer in this case, we need a certain initial *d*-spacing of clay, the right viscosity of resin, velocity of mixer to begin with. In other words, we need to increase the clay layer separation by another process prior to premixing with this mixer. This model can also be used to design a new mixer to give the desired shearing force.

NOMENCLATURE

ρ	Density of molecules in the block
ε	Relative dielectric permittivity or the dielectric constant
δ	Thickness of the clay plates, blocks
Ω	Velocity of cylinder mixer
ε_0	Electric permittivity of vacuum
a	Polarizability of the atom
A	Surface area of clay
D_r	Rotary diffusivity
F	Force vector acting on surface of clay
h	Distance between the surfaces of the clay plates, blocks
H_{11}	Hamaker constant
h_p	Planck's constant
M	Molecular weight of molecules in the block
N_{AV}	Avogadro's number
Pe	Peclet number
R_{12}	Intermolecular distance
R_i	Radii of inner wetted surface of coaxial cylinder
R_o	Radii of outer wetted surface of coaxial cylinder

References

1. Oh, T.-K.; Hassan, M.; Beatty, C.; El-Shall, H. J Appl Polym Sci 2006, 100, 3465.
2. Wang, H.; Hoa, S. V.; Wood-Adams, P. M. J Appl Polym Sci 2006, 100, 4286.
3. Lai, M.; Kim, J.-K. Polymer 2005, 46, 4722.
4. Lan, T.; Kaviratna, P. D.; Pinnavaia, T. J. Chem Mater 1995, 7, 2144.
5. Chin, I.-J.; Thurn-Albrecht, T.; Kim, H.-C.; Russell, T. P.; Wang, J. Polymer 2001, 42, 5947.
6. Ngo, T.-D.; Ton-That, M.-T.; Hoa, S. V.; Cole, K. C. Compos Sci Technol 2009, 69, 1831.
7. Ngo, T.-D.; Ton-That, M.-T.; Hoa, S. V.; Cole, K. C. Polym Eng Sci 2009, 49, 666.
8. Theng, B. K. G. The Chemistry of Clay-Organic Reactions; Wiley: New York, 1974.
9. Giannelis, E. P.; Krishnamoorti, R.; Manias, E. Adv Polym Sci 1999, 138, 107.
10. Sinha Ray, S.; Okamoto, M. Prog Polym Sci 2003, 28, 1539.
11. Sinha Ray, S.; Bousmina, M. Prog Mater Sci 2005, 50, 962.
12. Alexandre, M.; Dubois, P. Mater Sci Eng 2000, 28, 1.

13. Manias, E.; Touny, A.; Wu, L.; Strawhecker, K.; Lu, B.; Chung, T. C. Chem Mater 2001, 13, 3516.
14. Stokes, R. J.; Evans, D. F. Fundamentals of Interfacial Engineering; Wiley-VCH; Canada, 1997.
15. Hiemenz, P. C.; Rajagopalan, R. Principle of Colloid and Surface Chemistry; Marcel Dekker; New York, 1997.
16. Grimshaw, R. W. The Chemistry and Physics of Clays; Wiley: New York, 1971.
17. Recktenwald, A.; Lucke, M.; Muller, H. W. Phys Rev E 1993, 48, 4444.
18. Morrison, F. A. Understanding Rheology; Oxford Univ. Press: New York, 2001.
19. Bird, R. B.; Stewart, W. E.; Lightfoot, E. N.; Transport Phenomena; Wiley: New York, 1960.
20. Larson, R. G. The Structure and Rheology of Complex Fluids; Oxford University Press: New York, 1999.
21. Jeffery, G. B. Proc R Soc Lond A 1922, 102, 161.
22. Utracki, L. A. Clay-Containing Polymeric Nanocomposites; Rapra Technology; UK, 2004.
23. Kim, K.; Utracki, L. A.; Kamal, M. R. J Chem Phys 2004, 121, 10766.
24. Vial, J.; Carré, A. Int J Adhes Adhes 1991, 11, 140.
25. Médout-Marère, V. J Colloid Interface Sci 2000, 228, 434.